Evolutionary Ecology Research, 2006, **8**: 659–675

The impact of host longevity on disease transmission: host–pathogen dynamics and the evolution of resistance

Ulla Carlsson-Granér[1]* and Peter H. Thrall[2]

[1]*Department of Ecology and Environmental Science, Umeå University, SE-901 87 Umeå, Sweden and* [2]*CSIRO Plant Industry, Centre for Plant Biodiversity Research, GPO Box 1600, Canberra, ACT 2601, Australia*

ABSTRACT

Questions: How do disease transmission rates, host longevity, and spatial structure interact to determine disease dynamics and evolution of host resistance in systems where host sterility is the major consequence of infection?

Features of model: A spatially explicit two-dimensional simulation model with deterministic within-population birth and death processes, but stochastic among-population dispersal. The model assumes frequency-dependent disease transmission, and is loosely based on the pollinator-transmitted anther-smut fungus *Microbotryum violaceum*, which infects and sterilizes host plants in the Caryophyllaceae. Resistance varies among host individuals and is associated with a fitness cost.

Ranges of key variables: Simulations were run over ranges of host death rates, disease transmission rates, and spatial structures observed in natural host species.

Conclusions: The simulation model predicts that: (i) increasing host longevity and connectivity of host patches is likely to select for pathogen strains with lower transmission rates; (ii) when hosts are short-lived or populations are isolated, susceptible genotypes with higher reproductive output may have a selective advantage even when disease is widespread; (iii) when hosts are longer-lived or populations are more connected, resistance costs are lower and resistance can evolve to higher levels. Existing data from natural host–pathogen systems support these conclusions, although predictions about resistance patterns need to be tested in future studies.

Keywords: disease dynamics, disease transmission, evolution of resistance, host longevity, *Microbotryum violaceum*, spatial structure, sterilizing pathogen.

INTRODUCTION

For horizontally transmitted pathogens that rely on single host species for survival, theoretical models have shown that the ability of a pathogen to invade and persist increases with lower intrinsic host mortality (Anderson and May, 1982). Persistence on short-lived hosts with high natural death rates therefore requires higher transmission rates, and if transmission is positively correlated with pathogen virulence (i.e. the negative effect of infection on

* Author to whom all correspondence should be addressed. e-mail: ulla.carlsson-graner@emg.umu.se

host fitness), as generally assumed in epidemiological models, more aggressive pathogen strategies may be favoured under some conditions (Anderson and May, 1982; Lenski and May, 1994; Ebert and Herre, 1996; Gandon *et al.*, 2001). Pathogen persistence and the evolution of disease transmission rates may also depend on the spatial structure of host and pathogen populations (Haraguchi and Sasaki, 2000). For example, sterilizing pathogens that mainly affect host fitness by reducing host fecundity may evolve higher virulence (i.e. greater impact on host fecundity) in random mating populations, which sometimes drives the pathogen as well as the host towards extinction. In contrast, in spatially structured populations, the pathogen may evolve and persist at intermediate virulence and transmission rates (O'Keefe and Antonovics, 2002; O'Keefe, 2005).

While pathogen persistence is generally expected to be higher in spatially structured systems with partial connectivity than in isolated local populations (Antonovics *et al.*, 1994; Thrall and Antonovics, 1995; Hassell and Wilson, 1997; Thrall and Burdon, 1999; Carlsson-Granér and Thrall, 2002), spatial structure may influence disease dynamics differently in hosts with varying life-spans (cf. Kirchner and Roy, 1999). This is at least partly because the impact of host longevity on both recruitment rate and dispersal capacity, and rates of disease spread, are likely to be magnified in spatially structured systems (Franco and Silvertown, 1997; Olivieri and Gouyon, 1997; Kirchner and Roy, 1999).

Particularly in systems where hosts are sedentary, as in plant–pathogen interactions, host longevity could influence the persistence and turnover rates of local populations. If hosts are short-lived, both host and pathogen populations may be highly dynamic with frequent extinction and colonization events. Thus, in addition to higher local transmission rates, pathogen persistence is likely to require more efficient among-population dispersal. Moreover, with high turnover rates, chance founder effects during colonization may have large impacts on regional patterns of resistance and virulence (Frank, 1997; Thrall and Burdon, 1997; Carlsson-Granér and Pettersson, 2005). In longer-lived hosts, where population turnover rates are lower, the probability of an encounter between particular host and pathogen genotypes may be high, increasing the potential for reciprocal evolutionary changes in local host and pathogen populations (Burdon and Thrall, 1999; Thompson, 1999). If populations are connected through migration, these locally generated adaptations may spread through the system (Thompson, 1999).

The interactive effects of host and pathogen life-history attributes and spatial structure have been examined in a number of previous studies but the focus has generally been on the rates and mode of host and pathogen dispersal (Gandon *et al.*, 1996; Thrall and Burdon, 1999, 2002) or host life-history evolution (Kirchner and Roy, 1999). Here we use a simulation approach to examine how host longevity and disease transmission may interact to determine disease dynamics and the evolution of host resistance in spatially structured situations. We focus on pathogens that reduce host fecundity because spatial structure is predicted to be particularly important in such systems (cf. O'Keefe, 2005). Pathogens with fecundity effects are also less well studied than pathogens that increase host mortality (Antonovics, 2005) despite their potentially greater effect on host population size (Boots and Sasaki, 2002). The simulation model is loosely based on the pollinator-transmitted anther-smut fungus *Microbotryum violaceum* (Ustilaginales; syn. *Ustilago violacea*), which systemically infects and sterilizes a broad range of perennial plant species within the plant family Caryophyllaceae (Thrall *et al.*, 1993), but the broad conclusions of this study are likely to apply to many obligate natural host–pathogen interactions where host sterility is the major consequence of infection.

Theoretical and empirical studies suggest that the threshold disease transmission rates required for the initial increase of sterilizing pathogens decreases with increasing host longevity (Thrall *et al.*, 1993). However, the conditions for pathogen invasion may not be the same as the conditions for co-existence of host and pathogen (Gubbins *et al.*, 2000; O'Keefe and

Antonovics, 2002). Thus, while increasing the degree of among-population connectedness may initially result in greater disease spread (Hess, 1996a, 1996b), it may also increase the spread of host resistance alleles, which ultimately reduces average disease prevalence (Carlsson-Granér and Thrall, 2002). In the present study, we were specifically interested in evaluating how host death rate and disease transmission affect pathogen persistence, patterns of disease incidence and prevalence, and levels of resistance in metapopulations connected to different extents.

A major goal was to develop testable predictions that could be evaluated with empirical data. Anther-smut diseases have become a major model for studies of vector-transmitted plant diseases, thus data are available from a range of host–pathogen systems. The hosts of *M. violaceum* vary from very short-lived biennials through to very long-lived perennial species (Thrall *et al.*, 1993). This diversity of host life histories is matched by the wide range of spatial structures observed in different systems – for example, a linear roadside metapopulation of *Silene latifolia* in which patch turnover is relatively high (Thrall and Antonovics, 1995), relatively continuous to isolated populations of *Lychnis alpina* (Carlsson-Granér and Thrall, 2002), an island archipelago metapopulation with deterministic succession for *Silene dioica* (Carlsson and Elmqvist, 1992), and patchy relatively stable populations of *Silene acaulis* in open alpine areas (Marr and Delph, 2005).

METHODS

Simulation model structure

We used a spatially explicit two-dimensional simulation model in which the fraction of suitable host patches could be varied. The model structure is similar to that described in Carlsson-Granér and Thrall (2002) with deterministic population dynamics in local patches and stochastic distance-dependent among-patch dispersal of host and pathogen propagules. We assume that hosts vary in resistance [as demonstrated for several host species (Alexander *et al.*, 1996; Carlsson-Granér, 1997; Ouborg *et al.*, 2000)] and that resistance is determined by a single diploid locus with two alleles (i.e. host genotypes = SS, SR, and RR – ranging from fully susceptible to fully resistant) with heterozygotes exhibiting intermediate resistance. The pathogen is assumed to be genetically uniform [as is reasonable given the high degree of selfing (Kaltz and Shykoff, 1999; Hood and Antonovics, 2000) and the low genetic variability (Alexander *et al.*, 1996; Antonovics *et al.*, 1996; Carlsson-Granér, 1997; Kaltz *et al.*, 1999; Delmotte *et al.*, 1999; Ouborg *et al.*, 2000; Kaltz and Shykoff, 2002) observed in *M. violaceum*]. We further assume that infected hosts do not reproduce or recover, but that annual death rates (d) of healthy and diseased individuals are the same [as is frequently observed for pathogens or parasites that cause sterility (Antonovics, 2005)].

If we let $X_{\mathrm{SS}t}$, $X_{\mathrm{SR}t}$, $X_{\mathrm{RR}t}$, and Y_t represent the local numbers of susceptible, intermediate resistant, and resistant host genotypes, and the number of infected hosts at time t respectively (N_t is the total host population size in a local deme), and assuming a density-dependent birth rate, then the basic model for within-population host–pathogen dynamics can be written as:

$$X_{\mathrm{SS},t+1} = X_{\mathrm{SS},t}(1-d)(1-P_{\mathrm{SS}}) + \left[f_{\mathrm{S}}\left(X_{\mathrm{SS},t}\,\lambda_{\mathrm{SS}} + \frac{1}{2}X_{\mathrm{SR},t}\,\lambda_{\mathrm{SR}}\right)\right]\frac{1}{1+\gamma N_t} \quad (1)$$

$$X_{\mathrm{SR},t+1} = X_{\mathrm{SR},t}(1-d)(1-P_{\mathrm{SR}}) + \left(f_{\mathrm{S}}X_{\mathrm{RR},t}\lambda_{\mathrm{RR}} + f_{\mathrm{R}}X_{\mathrm{SS},t}\lambda_{\mathrm{SS}} + \frac{1}{2}X_{\mathrm{SR},t}\lambda_{\mathrm{SR}}\right)\frac{1}{1+\gamma N_t} \quad (2)$$

$$X_{\mathbf{RR},t+1} = X_{\mathbf{RR},t}(1-d)(1-P_{\mathbf{RR}}) + \left[f_{\mathbf{R}}\left(X_{\mathbf{RR},t}\lambda_{\mathbf{RR}} + \frac{1}{2}X_{\mathbf{SR},t}\lambda_{\mathbf{RR}}\right)\right]\frac{1}{1+\gamma N_t} \quad (3)$$

$$Y_{t+1} = \left(Y_t + \sum_i P_i X_{i,t}\right)(1-d) \quad (4)$$

The probability that an individual of a given genotype becomes diseased is given by P_i. The parameters $f_{\mathbf{S}}$ and $f_{\mathbf{R}}$ represent the local frequencies of S and R pollen respectively (including dispersal from other populations), while λ_i is the maximum annual per-capita reproductive rate (number of new individuals produced per adult plant) of the $i^{\mathbf{th}}$ host genotype (γ is a constant that determines the strength of density dependence). We included a cost of resistance by holding the reproductive rates (λ_i) for susceptible (SS) and resistant (RR) individuals constant at 3.5 and 2.5 respectively over all simulations. These values correspond to empirically estimated rates of annual per-capita reproduction in susceptible and resistant caryophyllaceous hosts (Thrall and Jarosz, 1994b; Carlsson-Granér and Thrall, 2002; Carlsson-Granér, 2006; Biere and Antonovics, 1996). Heterozygotes (SR) were assumed to have intermediate rates of reproduction. In the simulations, the annual death rate (d) was varied between 0.05 (long-lived perennial) and 0.75 (biennial–annual), which corresponds to the range of life-histories in caryophyllaceous hosts of anther smuts (Thrall *et al.*, 1993).

We assumed frequency-dependent non-linear disease transmission (cf. Antonovics *et al.*, 1997) in general agreement with patterns of disease spread in vector and sexually transmitted diseases (Antonovics, 2005). Thus the probability that a healthy plant becomes diseased (P_i) is given by:

$$P_i = 1 - \exp\left(-\beta_i \frac{Y_i}{N_i}\right) \quad (5)$$

where β_i is a parameter representing the effectiveness of disease transmission for the $i^{\mathbf{th}}$ host genotype. We held the transmission parameter ($\beta_{\mathbf{RR}}$) constant at 0.3 for resistant genotypes, while $\beta_{\mathbf{SS}}$ was varied between 0.5 and 7.5 for susceptible genotypes, corresponding to transmission rates estimated from different anther-smut hosts (Table 1; heterozygotes were assumed to have intermediate transmission rates). For $\beta_{\mathbf{SS}} = 0.5$ the probability that a healthy plant becomes diseased is relatively low, whereas for $\beta_{\mathbf{SS}} = 7.5$ the infection risk is very high (e.g. with 5% disease in a population, an annual infection rate of 31% is expected; see equation 5).

Model structure consisted of a two-dimensional array of patches (100×100) with absorbing boundaries (representative of metapopulations of definite size beyond which propagules are essentially lost from the system). We varied among-population connectedness by running simulations where 5, 10, or 50% of the patches were randomly allocated as suitable for host occupancy [the remaining patches were assigned a carrying capacity of 0 (see Carlsson-Granér and Thrall, 2002)]. Thus, with 5% habitat suitability, local host populations are quite isolated, while 50% habitat suitability corresponds to a situation where populations are relatively continuously distributed in that among-population dispersal occurs with high frequency. Simulations were initiated with 50% of the suitable habitat patches being randomly occupied by the host, with the R allele present at a frequency of 0.05. Carrying capacities of occupied patches were randomly assigned from a log-normal distribution with a mean of 50 (these were reassigned for each simulation run). Half of the initial host

Table 1. Life-history characteristics of some host systems of *Microbotryum violaceum* based on studies of natural populations

Host	Study site	Annual death rate (%)	Annual disease spread (%)	Transmission rate (S/R)*	Spatial structure of populations	Disease incidence (%)	Disease prevalence (%)
Silene rupestris	Sweden	60 (15–84)[1]	24–40[1]	5.8/0.3[1]	Patchy	N.D.	N.D.
Silene latifolia	USA	55 (30–83)[2,3,4]	4–24[2,4]	5.6/0.4[5]	Patchy (linear)	16–24[6]	24–42[6]
	Central Europe	N.D.	N.D.	N.D.	Patchy	N.D.	11–21[7,8,9]
	Netherlands	N.D.	N.D.	N.D.	Patchy	N.D.	9–12[10]
	Great Britain	N.D.	N.D.	N.D.	N.D.	76[11]	39[11]
Silene virginica	USA	39 (24–70)[12]	6–14[13]	N.D.	Patchy	67–78[13]	20–30[13]
Lychnis alpina	Sweden	29 (3–46)[14,15]	1–20[14,15]	2.4/0.3[14,15]	Isolated	9[14,15]	26–30[14,15]
					Patchy	60–66[14,15]	14–16[14,15]
					Continuous	67–75[14,15]	7–9[14,15]
Silene dioica	Sweden	18 (10–32)[16,17]	1–8[16,17]	1.0/0.2[17]	Patchy	65–75[16,17]	8–14[16,17]
	England		N.D.	N.D.	N.D.	90[18]	12[18]
Lychnis viscaria	Sweden	17 (8–27)[19,20]	1–3[19]	N.D.	Isolated	31–62[19,20]	8–16[19,20]
					Patchy	56–82[19,20]	23–27[19,20]
Silene acaulis	USA, Canada	1[21]	0–2.3[21,22]	N.D.	Patchy	71[23]	5–16[21,22,23]

Note: When possible the following estimates are given: annual host death rates [overall average, min and max (within parentheses)], annual disease spread (range among years), estimated disease transmission rates of susceptible (S) and resistant (R) genotypes (assuming frequency-dependent non-linear disease transmission), disease incidence (fraction diseased populations) (range among years), average disease prevalence in diseased populations (range among years), and spatial structure of populations. Spatial structure was determined as 'isolated' when the reported distances between populations were large, as 'patchy' in systems where populations were defined as metapopulations or patchily distributed, and as 'continuous' in one case where populations were distributed throughout the studied area. N.D. = no data.

* Transmission rates were estimated from equation (5).

Italic superscript numerals refer to data sources: *1*, Carlsson-Granér (2006); *2*, Alexander and Antonovics (1988); *3*, Thrall and Jarosz (1994a); *4*, Alexander and Antonovics (1995); *5*, Antonovics *et al.* (1997); *6*, Thrall and Antonovics (1995); *7*, Kaltz *et al.* (1999); *8*, Bucheli *et al.* (2001); *9*, Kaltz and Shykoff (2001); *10*, Ouborg *et al.* (2000); *11*, Baker (1947); *12*, Dudash and Fenster (1997); *13*, Antonovics *et al.* (1996); *14*, Carlsson-Granér and Thrall (2002); *15*, U. Carlsson-Granér (unpublished data); *16*, Carlsson and Elmqvist (1992); *17*, U. Carlsson-Granér and B.E. Giles (unpublished data); *18*, Lee (1981); *19*, Jennersten *et al.* (1983); *20*, Jennersten (1985); *21*, Marr and Delph (2005); *22*, Marr (1997); *23*, Hermanutz and Innes (1994).

populations were then randomly chosen to have the pathogen present at a frequency of 0.1 (i.e. 10% of hosts infected in these populations).

In each generation (= 1 year), a fraction each of the spores, pollen, and seeds produced in each population were dispersed according to a negative exponential function (see Thrall and Antonovics, 1995; Thrall and Burdon, 1999, 2002), with a maximum dispersal distance of 5 units for both host and pathogen. Such distance-dependent pathogen dispersal has been empirically demonstrated for *M. violaceum* (Antonovics *et al.*, 1994; Pettersson *et al.*, 2000; Marr and Delph, 2005) as well as for a number of other plant–pathogen systems (Burdon *et al.*, 1995; Ericson *et al.*, 1999; Thrall *et al.*, 2003). The probability of infection within a local population is thus a function of spores immigrating from other diseased populations as well as the fraction of diseased hosts already present. Host population growth was similarly dependent on both within-population reproduction and immigration of seeds from other patches.

Over-winter adult death occurred subsequent to infection, reproduction, dispersal, and establishment of new host and pathogen populations. Before the within-population dynamics phase, a probability of extinction was calculated for each occupied patch as a function of population size (cf. Thrall and Antonovics, 1995). Disease was permanently lost from the system when the pathogen went extinct in all local populations. For each scenario investigated (representing different combinations of spatial distributions of host populations, host death rate, and disease transmission), 50 replicate runs of 1000 generations were performed (at 1000 generations both numerical and genetic dynamics had generally stabilized). To track dynamical changes and persistence times of host and pathogen, data were collected each generation on the fraction of suitable patches occupied, fraction of host patches with disease present (incidence), average disease prevalence, and frequency of the R allele across the metapopulation. Individual population data were collected at the end of simulation runs to examine the dependence of host resistance and disease incidence/prevalence patterns on spatial structure in hosts with different life-spans.

SIMULATION RESULTS

Pathogen persistence

Over all spatial scales, there were significant interactions between host life-span, disease transmission rates, and the probability of long-term pathogen persistence. In general, greater host death rates required higher disease transmission rates among susceptible hosts for equilibrium persistence of the pathogen (i.e. over the 1000 generations that simulations ran; Fig. 1). The mean transmission rates observed across all host genotypes in the system at equilibrium also increased with host death rate (Fig. 2). The evolution of increased resistance, particularly in longer-lived hosts (Fig. 3), meant that the mean disease transmission rate observed in the system at equilibrium was generally lower (Fig. 2) than the transmission rate for the susceptible genotype (see Fig. 1).

In short-lived hosts ($d \geq 0.5$), long-term pathogen persistence was possible at all spatial scales, although a somewhat higher transmission rate among susceptible hosts was required for long-term persistence in more fragmented systems (i.e. a lower percentage of suitable host patches; Fig. 1). In contrast, for host death rates <0.5, long-term persistence of the pathogen only occurred when local host populations were less isolated (Figs. 1b, c, 2). Moreover, within this range of death rates, patterns of pathogen persistence changed considerably when the fraction of suitable habitat patches was increased. For relatively

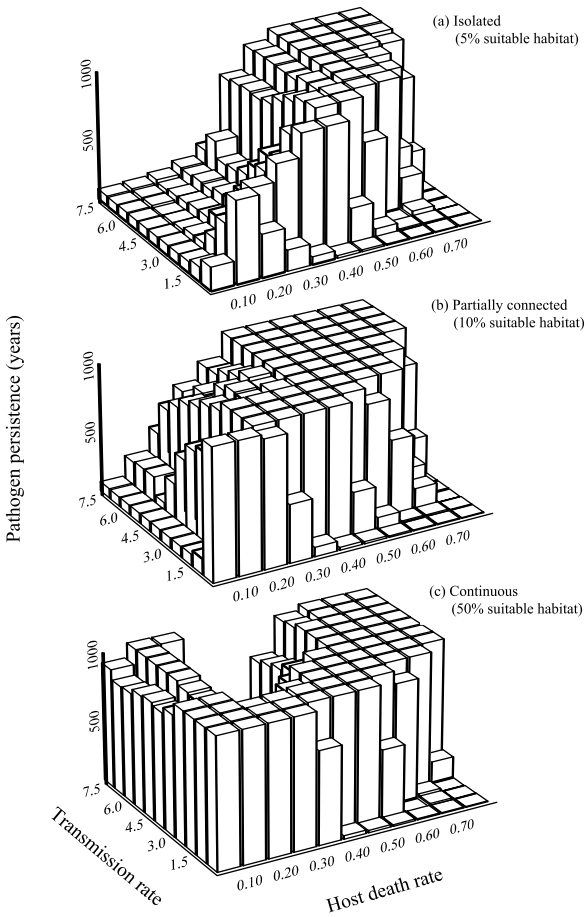

Fig. 1. The relationship between pathogen persistence (number of generations the pathogen persisted in simulations), host death rate, and disease transmission rate of the susceptible genotype for different levels of among-population connectedness (as determined by the percentage of habitat that can be occupied by the host). Bars represent the mean of 50 random runs for a maximum of 1000 generations.

long-lived hosts ($d \leq 0.15$), pathogen persistence decreased with transmission rate in isolated (Fig. 1a) and partially connected (Fig. 1b) situations. However, when the distribution of host populations was more continuous, the pathogen persisted for long periods of time even when susceptible transmission rates were very high (Fig. 1c). In this case, particularly when hosts were long-lived, the resistant allele was nearly always close to fixation (Fig. 3c). For intermediate mortality rates ($d = 0.2$–0.3), the probability of long-term pathogen persistence was greatest in partially connected systems (Fig. 1b).

Patterns of resistance

In very short-lived hosts ($d = 0.75$), the frequency of resistance was always at or near zero at equilibrium regardless of the percentage of suitable habitats, disease transmission rates, or levels of disease across the metapopulation. In contrast, in hosts with lower death rates,

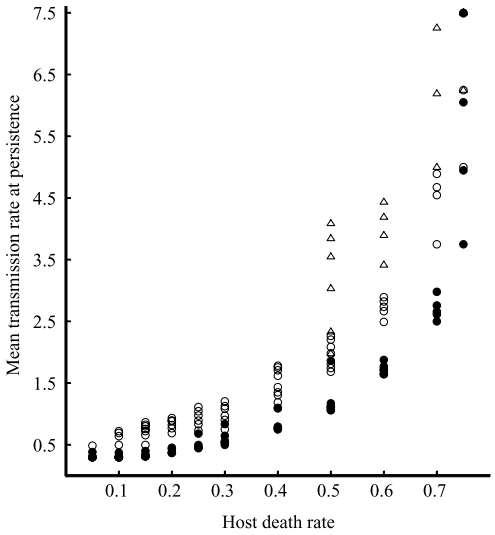

Fig. 2. Mean disease transmission rate across the metapopulation for parameter values permitting long-term pathogen persistence as a function of host death rate and the degree of among-population connectedness. In the simulations, the percentage of suitable patches is 5% (△), 10% (○), and 50% (●). Each point represents the mean of 50 random runs where the pathogen was still present after 1000 generations.

resistance generally increased with disease transmission rates as long as the pathogen remained in the system (Fig. 3).

With respect to spatial structure, higher resistance evolved with increasing among-population connectedness (Fig. 3a–c). For partially connected or continuous host populations, within the ranges of host death rates and disease transmission rates where long-term pathogen persistence was possible, the frequency of resistance was always higher in longer-lived hosts (Fig. 3b, c). In the most connected situation, resistance actually evolved to fixation for very long-lived hosts ($d = 0.05$; Fig. 3c). Whenever the pathogen went extinct, the frequency of resistance always decreased over time but it could take a long time (up to 3000 generations – data not shown), especially in very long-lived hosts ($d = 0.05$) and in situations with a greater degree of connectivity among local populations.

Disease incidence and disease prevalence

Figure 4 shows disease incidences (fraction of populations with disease) and disease prevalences (frequency of diseased individuals in populations) observed at equilibrium over the range of disease transmission rates where long-term pathogen persistence was possible (see Fig. 1). On average, more populations were diseased when a greater proportion of the habitat was suitable for the host (Fig. 4a). In isolated (5% suitable habitat) and partially connected situations (10% suitability), disease incidences tended to be higher in shorter-lived hosts (Fig. 4a). In continuous populations (50% suitability), the levels of disease incidence observed in hosts with different life-spans overlapped to a much greater extent (Fig. 4a). In contrast to patterns of disease incidence, lower levels of disease prevalence were observed when host habitat availability was greatest (Fig. 4b). Disease prevalence also

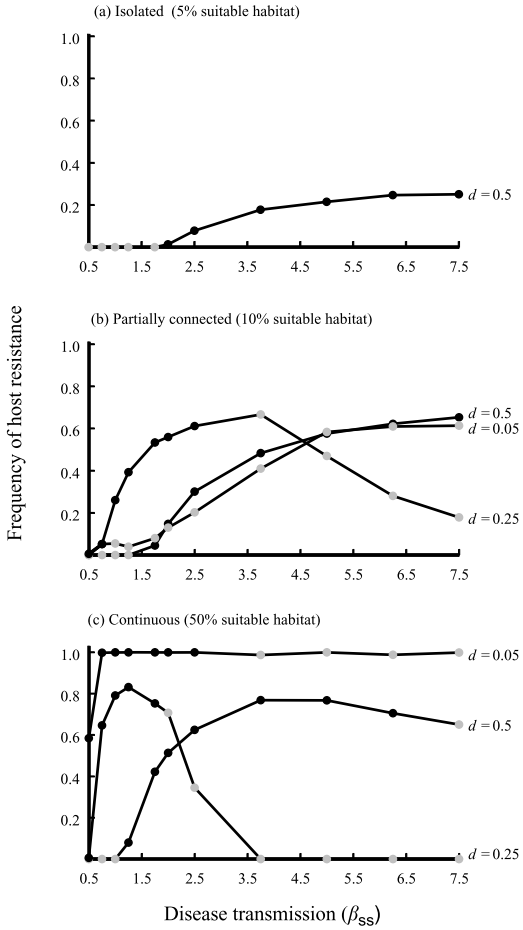

Fig. 3. The average frequency of host resistance across the metapopulation at 1000 generations for hosts with death rates of 0.05, 0.25, and 0.5, respectively, as a function of the disease transmission rate of the susceptible genotype. Black circles represent parameter ranges for which a long-term pathogen persistence was possible, while grey circles indicate parameter values that resulted in the pathogen going extinct in less than 1000 generations (see Fig. 1). Each point represents the mean of 50 random runs at 1000 generations.

tended to decrease with increasing host death rate, especially in more fragmented situations (i.e. 5 and 10% habitat suitability; Fig. 4b). In the most connected situation, however, increasing the host death rate beyond 0.7 resulted in slightly higher equilibrium levels of disease prevalence (Fig 4b).

Comparison of model predictions with data from natural host populations

Table 1 summarizes data from several host species of *M. violaceum* where death rates, rates of disease spread, and patterns of disease incidence and prevalence have been quantified. For *S. acaulis*, *S. dioica*, *S. latifolia*, and *L. alpina*, data are available from many populations

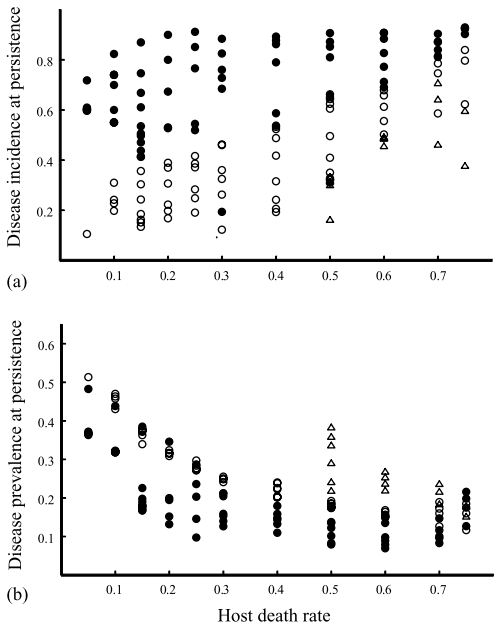

Fig. 4. Disease incidence (fraction of diseased patches) and average disease prevalence across the metapopulation after 1000 generations, within the range of disease transmission rates where long-term pathogen persistence occurred (see Fig. 1), as a function of host death rate. In the simulations, the percentage of suitable patches is 5% (△), 10% (○), and 50% (●). Each point represents the mean of 50 random runs at 1000 generations.

over multiple years, with similar data over at least 2 years for the hosts *Lychnis viscaria* and *Silene virginica*, and over several years in one population of *Silene rupestris* (Table 1).

In agreement with simulation predictions, data on disease spread from several host species suggest that average transmission rates vary inversely with host life-span. The highest disease transmission rates for susceptible individuals have been observed in the relatively short-lived hosts *S. latifolia* and *S. rupestris*, while transmission rates are considerably lower in populations of the longer-lived *L. alpina* and *S. dioica* (Table 1). For the other host species of *M. violaceum*, it was not possible to estimate disease transmission rates as data on annual infection rates in relation to disease frequency in single populations were unavailable. However, average annual rates of disease spread are reported to be extremely low in the very long-lived *S. acaulis* as well as in the relatively long-lived *L. viscaria* (Table 1).

One expectation from the simulations is that the degree of among-population connectedness will be positively related to disease incidence, but negatively related to prevalence (Fig. 4). Empirical studies of anther-smut infection in two hosts, *L. alpina* and *L. viscaria*, are consistent with this prediction – in regions where populations are more isolated, disease incidence is generally lower than in more continuously inhabited areas (Table 1) (Carlsson-Granér and Thrall, 2002). Moreover, in *L. alpina* higher disease prevalence has been observed in more isolated populations compared with more continuous situations. However, for most of the studied host species it is not possible to compare patterns of disease in relation to the spatial structure of host populations, as data on inter-population distances are generally missing or are difficult to interpret. For example, systems classified as patchy may represent

a variety of spatial structures where actual distances between populations vary. Spatial structure aside, the ranges of average disease incidence and disease prevalence estimated from natural systems (Table 1) overlap in general with the ranges predicted for hosts with corresponding death rates in the simulation (Fig. 4a, b). The exception is *S. acaulis*, for which the estimated disease prevalence in natural populations is lower on average than that seen in the simulation (Fig. 4b). Recent work suggests that the rarity of vegetative infection of juveniles and the short flowering time in *S. acaulis* in comparison with other host species may contribute to low rates of disease spread (Marr and Delph, 2005).

DISCUSSION

Host longevity and disease transmission rates

In accordance with a previous model (Thrall *et al.*, 1993), in our simulations the threshold disease transmission rate above which the pathogen persisted generally increased with increasing intrinsic death rates of the host. Because resistance evolved to higher frequencies in longer-lived hosts, the mean transmission rate after 1000 generations was always lower than in shorter-lived hosts. Although data on disease transmission rates from natural anther-smut diseased host populations is rather limited, the available data are in accordance with the simulation results. Thus, the highest disease transmission rates for susceptible individuals have been observed in the relatively short-lived hosts *S. rupestris* and *S. latifolia*, while transmission rates are considerably lower in the longer-lived *L. alpina* and *S. dioica*. Low rates of disease spread have also been observed in the very long-lived host *S. acaulis* and in the relatively long-lived *L. viscaria* (Table 1), suggesting that strains with lower transmission rates may be favoured in longer-lived hosts. Consistent with this idea, Van Putten *et al.* (2003) recently found that anther-smut strains from *S. dioica* had lower conjugation-frequencies and infection success but also longer latency periods than strains from the shorter-lived *S. latifolia*.

For systemic diseases that impact on host fecundity rather than mortality, particularly for longer-lived host species, infected plants represent perennial inoculum sources that are generally unavailable for new infections (Marr and Delph, 2005). At the same time, because diseased plants are sterile, few new healthy hosts will establish in highly diseased populations. Such negative impacts on population growth are predicted for pathogens with fecundity effects (Boots and Sasaki, 2002) and have been documented for at least some anther-smut hosts (Carlsson and Elmqvist, 1992; Antonovics *et al.*, 1994). Our results were consistent with this prediction – negative effects of infection on growth were strongest in simulations with long-lived hosts ($d < 0.15$), where the disease initially reached very high incidence and prevalence across the metapopulation, after which there was a sharp decrease in levels of disease as well as in host occupancy (data not shown). However, the severity of the population decline also depended on the rate at which host resistance evolved (most rapid for higher transmission rates). Because resistance is associated with a fitness cost (resistant hosts produce fewer progeny than susceptible ones), a high frequency of resistance will not only decrease disease levels but will also lower the growth rate of local populations. With higher transmission rates, the pathogen may drive itself locally extinct before being transmitted to another patch of healthy hosts. Thus, although higher transmission rates will generally be favoured in well-mixed local populations, especially for sterilizing diseases where there is no fitness cost associated with high transmission, pathogens with lower transmission rates can

persist in spatially structured systems (Haraguchi and Sasaki, 2000; O'Keefe and Antonovics, 2002; Boots *et al.*, 2003).

In simulations with short-lived perennial hosts ($d \geq 0.5$), pathogen persistence required high transmission rates to balance the yearly loss of diseased plants. While high transmission rates resulted in the pathogen spreading to a very large fraction of populations, continual population turnover provided opportunities for establishment and colonization of new healthy hosts. Thus, disease prevalence was lower, and the fraction of patches occupied higher, than for longer-lived hosts where population turnover was less dynamic. In short-lived hosts, high turnover may also prevent resistance from evolving to high frequencies, as local extinction of either the host or the pathogen may occur faster than pathogen-mediated selection can change the genetic composition of populations (Thrall and Antonovics, 1995; Frank, 1997). The costs of lower seed production in resistant plants will also be greatest in shorter-lived hosts where high seed production and dispersal are likely to be critical for regional persistence (Olivieri and Gouyon, 1997; Carlsson-Granér and Pettersson, 2005). This could explain why resistance never evolved in diseased populations in the most short-lived host system investigated in our simulation.

For pathogens that affect host mortality rather than fecundity, high intrinsic host mortality rates may also favour high transmission rates and thus high virulence (e.g. Anderson and May, 1982; Ebert and Herre, 1996). However, pathogen transmission may not always be maximized. For example, if super-infection is possible (i.e. when an infected host can be re-infected by a new pathogen strain), pathogens may evolve lower virulence and transmission rates with greater host death rates (Ebert and Mangin, 1997; Gandon *et al.*, 2001). This is because high host mortality decreases the intensity of within-host competition, which counteracts selection for increased virulence (Gandon *et al.*, 2001).

The importance of spatial structure

The increasing subdivision of host populations into smaller, more isolated patches will slow among-patch dispersal rates and is therefore likely to increase the probability of local extinction of the pathogen (Thrall and Antonovics, 1995; Nee *et al.*, 1997). In our simulations, as the degree of among-population isolation increased, the range of host death rates over which the pathogen persisted declined and higher disease transmission rates were required for long-term pathogen persistence. In fact, in the most isolated situation (5% suitable sites), long-term disease persistence was only possible in relatively short-lived hosts. Although the disease transmission threshold was always higher for shorter-lived hosts, connectedness reduced the dependence of pathogen persistence on host longevity. When host patches are more connected, pathogen spread among populations may lead to damped fluctuations in local abundance and long-term persistence of pathogen populations is more easily achieved (Thrall and Antonovics, 1995; Hassell and Wilson, 1997; Thrall and Burdon, 1999; Carlsson-Granér and Thrall, 2002). In our simulation, the fraction of diseased populations generally increased when host patches became more connected and this pattern was most evident in longer-lived hosts. In contrast, disease prevalence within populations was on average lower in more connected patch systems because of the higher equilibrium levels of host resistance that evolved (see also Carlsson-Granér and Thrall, 2002), particularly in longer-lived hosts.

Assuming a cost of resistance, one consequence of the higher proportion of susceptible individuals in short-lived hosts is a higher average per-capita reproduction rate. This may result in higher plant colonization rates (Olivieri and Gouyon, 1997) and in our simulations

shorter-lived hosts were always able to occupy a larger fraction of the patches than longer-lived hosts. Such situations (increased patch occupancy for a given level of fragmentation, higher proportion of newly founded populations being susceptible) may also result in higher disease colonization rates (Antonovics *et al.*, 1997). This could explain why long-term pathogen persistence in fragmented situations occurred more readily in shorter-lived host systems. In longer-lived hosts, where resistance initially always evolved to high frequencies, the mean disease transmission rate was probably too low to balance local pathogen extinctions in the most isolated situations.

As predicted by deterministic models (Thrall and Jarosz, 1994b), in our simulations the combination of relatively high host turnover ($0.25 \leq d \leq 0.4$) and high resistance in the most connected situation led to loss of the pathogen over a large range of transmission rates. Within this range of host life-spans, the probability of pathogen persistence actually increased as the metapopulation became more fragmented (i.e. at 10% habitat suitability). When populations are only partially connected and the turnover rate of populations is relatively high, metapopulation dynamics may be most important. Similarly, when the spatial extent of among-population pathogen dispersal is relatively local, pathogen persistence may be maximized (Thrall and Burdon, 1999). Thus, founder effects associated with colonization and extinction processes, among-population asynchrony in disease dynamics, and opposing selection on host resistance during colonization and growth of populations all contribute to maintenance of variation for resistance (Frank, 1997; Burdon and Thrall, 1999; Carlsson-Granér and Pettersson, 2005), which can mediate host–pathogen co-existence at the metapopulation level (Thrall and Antonovics, 1995; Antonovics *et al.*, 1997).

The ranges of disease incidence and prevalence observed in natural systems (Table 1) generally overlap with predicted ranges for hosts with corresponding death rates in the simulation (Fig. 4a, b). Moreover, similar to patterns generated in the simulations, studies of *L. alpina* and *L. viscaria* have found that the fraction of diseased populations is higher in areas where populations are more connected (Table 1). However, while we have some knowledge about patterns of resistance in patchy metapopulations in two hosts, *S. dioica* and *S. latifolia* (Thrall and Antonovics, 1995; Alexander *et al.*, 1996; Carlsson-Granér, 1997; Carlsson-Granér and Pettersson, 2005), information on spatial structure, resistance frequency, and patterns of disease is generally lacking for natural systems. Our simulations suggest that the highest levels of resistance are likely to occur in relatively long-lived hosts or where local populations are well-connected by dispersal.

Pathogen impact on host abundance

Because increased contact among populations may enhance disease spread, it has been argued that conservation management should be cautious in advocating the establishment of wildlife corridors, or other strategies that permit greater movement of individuals among populations (Hess, 1996a, 1996b). However, increased pathogen dispersal (through greater connectivity of host populations) may also increase the potential for selection of resistance, which will ultimately lower disease levels and the negative impact of disease (McCallum and Dobson, 2002; Carlsson-Granér and Thrall, 2002). This highlights the need to incorporate both ecological and genetic factors in models of host–pathogen interactions, especially with regard to predictions about the impact of pathogens on host abundance.

Somewhat paradoxically, while the probability of pathogen persistence was lower in simulations with longer-lived hosts, especially in isolated situations, disease impact may be

more severe than in shorter-lived host species. In long-lived hosts, population growth rates decreased sharply as both disease prevalence and the frequency of resistance increased, which increases the risk of local host extinction despite the fact that the pathogen may ultimately be driven to extinction (O'Keefe and Antonovics, 2002). Similarly, Kirchner and Roy (1999) showed that, if long-lived hosts share the same risk of infection with short-lived species, selection can favour longer-lived hosts in isolated populations, which results in negative impacts on host growth. In metapopulation situations, selection may favour shorter-lived hosts and the impact of disease is smaller. In our simulations, the frequency of resistance generally declined and host growth rate increased as the pathogen declined towards extinction. However, because the rate of selection against resistant genotypes in the absence of disease is expected to be inversely related to population turnover rate and host generation time (Thrall and Antonovics, 1995), it sometimes took several thousand generations for resistance to be lost from disease-free populations of long-lived hosts.

GENERAL CONCLUSIONS

Our results suggest that in systems where host sterility is a major consequence of infection, increasing host longevity and/or connectivity of host patches is likely to select for pathogen strains with lower transmission rates. Moreover, when hosts are short-lived or populations are isolated, susceptible plants may disperse and colonize new patches more rapidly than resistant plants, giving susceptible genotypes a selective advantage even when disease is widespread (see also Bowers *et al.*, 1994; Boots and Haraguchi, 1999; Carlsson-Granér and Pettersson, 2005). When hosts are longer-lived or populations are more connected, resistance costs are lower because high reproduction and dispersal have less influence on local and regional dynamics (cf. Olivieri and Gouyon, 1997), and resistance can evolve to high levels. Overall, these results only begin to hint at the complex ways in which variation in host and pathogen life-history traits may interact with spatial structure to influence co-evolution in natural systems (see also Jarosz and Davelos, 1995; Thrall and Burdon, 1997; Thompson, 1999).

ACKNOWLEDGEMENTS

We thank J.J. Burdon, B.R. Levin, and two anonymous reviewers for comments on the manuscript and acknowledge the Wenner-Gren Foundation for supporting this work when P.H.T. was a visiting scientist at the Department of Ecology and Environmental Science, Umeå University. U.C.G. also acknowledges the support of the Carl-Fredrik von Horns Fund and the Swedish Research Council for Environment, Agricultural Sciences, and Spatial Planning (FORMAS).

REFERENCES

Alexander, H.M. and Antonovics, J. 1988. Disease spread and population dynamics of anther-smut infection of *Silene alba* caused by the fungus *Ustilago violacea*. *J. Ecol.*, **76**: 91–104.

Alexander, H.M. and Antonovics, J. 1995. Spread of anther-smut disease (*Ustilago violacea*) and character correlations in a genetically variable experimental population of *Silene alba*. *J. Ecol.*, **83**: 783–794.

Alexander, H.M., Thrall, P.H., Antonovics, J., Jarosz, A.M. and Oudemans, P.V. 1996. Population dynamics and genetics of plant diseases: a case study of anther-smut disease of *Silene alba* caused by the fungus *Ustilago violacea*. *Ecology*, **77**: 990–996.

Anderson, R.M. and May, R.M. 1982. Coevolution of hosts and parasites. *Parasitology*, **85**: 411–426.

Antonovics, J. 2005. Plant venereal disease: insight from a messy metaphor. *New Phytol.*, **165**: 71–80.

Antonovics, J., Thrall, P.H., Jarosz, A.M. and Stratton, D. 1994. Ecological genetics of metapopulations: the *Silene–Ustilago* plant–pathogen system. In *Ecological Genetics* (L. Real, ed.), pp. 146–170. Princeton, NJ: Princeton University Press.

Antonovics, J., Stratton, D., Thrall, P.H. and Jarosz, A.M. 1996. An anther-smut disease (*Ustilago violacea*) of Fire-pink (*Silene virginica*): its biology and relationship to the anther-smut disease of White Campion (*Silene alba*). *Am. Midl. Nat.*, **135**: 130–143.

Antonovics, J., Thrall, P.H. and Jarosz, A.M. 1997. Genetics and the spatial ecology of species interactions: the *Silene–Ustilago* system. In *Spatial Ecology: The Role of Space in Population Dynamics and Interspecific Interactions* (D. Tillman and P. Kareiva, eds,), pp. 158–180. Princeton, NJ: Princeton University Press.

Baker, H.G. 1947. Infection of species of *Melandrium* by *Ustilago violacea* (pers.) Fuckel and the transmission of the resultant disease. *Ann. Bot.*, **11**: 333–348.

Biere, A. and Antonovics, J. 1996. Sex specific costs of resistance to the fungal pathogen *Ustilago violacea* (*Microbotryum violaceum*) in *Silene alba*. *Evolution*, **50**: 1098–1110.

Boots, M. and Haraguchi, Y. 1999. The evolution of costly resistance in host–parasite systems. *Am. Nat.*, **153**: 359–370.

Boots, M. and Sasaki, A. 2002. Parasite driven extinction in spatially explicit host–parasite systems. *Am. Nat.*, **159**: 706–713.

Boots, M., Hudson, P.J. and Sasaki, A. 2003. Large shifts in pathogen virulence relate to host population structure. *Science*, **303**: 842–844.

Bowers, R.G., Boots, M. and Begon, M. 1994. Life-history trade-offs and the evolution of pathogen resistance: competition between host strains. *Proc. R. Soc. Lond. B*, **257**: 247–253.

Bucheli, E., Gautschi, B. and Shykoff, J.A. 2001. Differences in population structure of the anther-smut fungus *Microbotryum violaceum* on two closely related host species, *Silene latifolia* and *Silene dioica*. *Mol. Ecol.*, **10**: 285–294.

Burdon, J.J. and Thrall, P.H. 1999. Spatial and temporal patterns in coevolving plant and pathogen associations. *Am. Nat.*, **153**: S15–S33.

Burdon, J.J., Ericson, L. and Müller, W.J. 1995. Temporal and spatial changes in a metapopulation of the rust pathogen *Triphragmium ulmariae* and its host, *Filipendula ulmaria*. *J. Ecol.*, **83**: 979–989.

Carlsson-Granér, U. 1997. Anther-smut disease in *Silene dioica*: variation in susceptibility among genotypes and populations, and patterns of disease within populations. *Evolution*, **51**: 1416–1426.

Carlsson-Granér, U. 2006. Disease dynamics, host specificity and pathogen persistence in isolated host populations. *Oikos*, **112**: 174–184.

Carlsson, U. and Elmqvist, T. 1992. Epidemiology of anther-smut disease (*Microbotryum violaceum*) and numeric regulation of populations of *Silene dioica*. *Oecologia*, **90**: 509–517.

Carlsson-Granér, U. and Pettersson, T.M. 2005. Patterns of host susceptibility and disease occurence in a metapopulation of *Silene dioica*. *Evol. Ecol. Res.*, **7**: 353–369.

Carlsson-Granér, U. and Thrall, P.H. 2002. The spatial distribution of plant populations, disease dynamics and evolution of resistance. *Oikos*, **97**: 97–110.

Delmotte, F., Bucheli, E. and Shykoff, J.A. 1999. Host and parasite population structure in a natural plant–pathogen system. *Heredity*, **82**: 300–308.

Dudash, M.R. and Fenster, C.B. 1997. Multiyear study of pollen limitation and cost of reproduction in the iteroparous *Silene virginica*. *Ecology*, **78**: 484–493.

Ebert, D. and Herre, E.A. 1996. The evolution of parasitic diseases. *Parasitol. Today*, **12**: 96–101.

Ebert, D. and Mangin, K.L. 1997. The influence of host demography on the evolution of virulence of a microsporidian gut parasite. *Evolution*, **51**: 1828–1837.

Ericson, L., Burdon, J.J. and Muller, W.J. 1999. Spatial and temporal dynamics of epidemics of the rust fungus *Uromyces valerianae* on populations of its host *Valeriana salina*. *J. Ecol.*, **87**: 649–658.

Franco, M. and Silvertown, J. 1997. Life history variation in plants: an exploration of the fast–slow continuum hypothesis. In *Plant Life Histories* (J. Silvertown, M. Franco and J. Harper, eds.), pp. 210–227. Cambridge: Cambridge University Press.

Frank, S.A. 1997. Spatial processes in host–parasite genetics. In *Metapopulation Biology: Ecology, Genetics and Evolution* (I. Hanski and M.E. Gilpin, eds.), pp. 325–352. San Diego, CA: Academic Press.

Gandon, S., Capowiez, Y., Dubois, Y., Michalakis, Y. and Olivieri, I. 1996. Local adaptation and gene-for-gene coevolution in a metapopulation model. *Proc. R. Soc. Lond. B*, **263**: 1003–1009.

Gandon, S., Vincent, A.A. and van Baalen, M. 2001. Host life history and the evolution of parasite virulence. *Evolution*, **55**: 1056–1062.

Gubbins, S., Gilligan, C.A. and Kleczkowski, A. 2000. Population dynamics of plant–parasite interactions: threshold for invasion. *Theor. Pop. Biol.*, **57**: 219–233.

Haraguchi, Y. and Sasaki, A. 2000. The evolution of parasite virulence and transmission rate in spatially structured population. *J. Theor. Biol.*, **203**: 85–96.

Hassell, M.P. and Wilson, H.B. 1997. The dynamics of spatially distributed host–parasitoid systems. In *Spatial Ecology: The Role of Space in Population Dynamics and Interspecific Interactions* (D. Tilman and P. Kareiva, eds.), pp. 75–110. Princeton, NJ: Princeton University Press.

Hermanutz, L.A. and Innes, D.J. 1994. Gender variation in *Silene acaulis* (Caryophyllaceae). *Pl. Syst. Evol.*, **191**: 69–81.

Hess, G. 1996a. Disease in metapopulation models: implications for conservation. *Ecology*, **77**: 1617–1632.

Hess, G. 1996b. Linking extinction to connectivity and habitat destruction in metapopulation models. *Am. Nat.*, **148**: 226–236.

Hood, M.E. and Antonovics, J. 2000. Intratetrad mating, heterozygosity, and the maintenance of deleterious alleles in *Microbotryum violaceum* (= *Ustilago violacea*). *Heredity*, **85**: 231–241.

Jarosz, A.M. and Davelos, A.L. 1995. Effects of disease in wild populations and the evolution of pathogen aggressiveness. *New Phytol.*, **129**: 371–387.

Jennersten, O. 1985. Pollination and fungal disease transmission: interactions between *Viscaria vulgaris*, *Ustilago* and insects. PhD thesis, Department of Zoology, Uppsala University, Uppsala, Sweden.

Jennersten, O., Nilsson, S.G. and Wästljung, U. 1983. Local plant populations as ecological islands: the infection of *Viscaria vulgaris* by the fungus *Ustilago violacea*. *Oikos*, **41**: 391–395

Kaltz, O. and Shykoff, J.A. 1999. Selfing versus outcrossing propensity of the fungal pathogen *Microbotryum violaceum* across *Silene latifolia* host plants. *J. Evol. Biol.*, **12**: 340–349.

Kaltz, O. and Shykoff, J.A. 2001. Male and female *Silene latifolia* differ in per contact risk of infection by a sexually transmitted disease. *J. Ecol.*, **89**: 99–109.

Kaltz, O. and Shykoff, J.A. 2002. Within- and among-population variation in infectivity, latency and spore-production in a host–pathogen system. *J. Evol. Biol.*, **15**: 850–860.

Kaltz, O., Gandon, S., Michalakis, Y. and Shykoff, J.A. 1999. Local maladaptation in the anther-smut fungus *Microbotryum violaceum* to its host plant *Silene latifolia*: evidence from a cross-inoculation experiment. *Evolution*, **53**: 395–407.

Kirchner, J.W. and Roy, B.A. 1999. The evolutionary advantages of dying young: epidemiological implications of longevity in metapopulations. *Am. Nat.*, **154**: 140–159.

Lee, J.A. 1981. Variation in the infection of *Silene dioica* (L.) Clairv. by *Ustilago violacea* in north west England. *New Phytol.*, **87**: 81–89.

Lenski, R.E. and May, R.M. 1994. The evolution of virulence in parasites and pathogens: reconciliation between two competing hypotheses. *J. Theor. Biol.*, **100**: 411–426.

Marr, D.L. 1997. Impact of a pollinator-transmitted disease on reproduction in healthy *Silene acaulis*. *Ecology*, **78**: 1471–1480.

Marr, D.L. and Delph, L.F. 2005. Spatial and temporal patterns of a pollinator-transmitted pathogen in a long-lived perennial (*Silene acaulis*). *Evol. Ecol. Res.*, **7**: 335–352.

McCallum, H. and Dobson, A. 2002. Disease, habitat fragmentation and conservation. *Proc. R. Soc. Lond. B*, **269**: 2041–2049.

Nee, S., May, R.M. and Hassell, M.P. 1997. Two-species metapopulations models. In *Metapopulation Biology: Ecology, Genetics and Evolution* (I. Hanski and M.E. Gilpin, eds.), pp. 123–147. San Diego, CA: Academic Press.

O'Keefe, K.J. 2005. The evolution of virulence in pathogens with frequency-dependent transmission. *J. Theor. Biol.*, **233**: 55–64.

O'Keefe, K.J and Antonovics, J. 2002. Playing by different rules: the evolution of virulence in sterilizing pathogens. *Am. Nat.*, **159**: 597–605.

Olivieri, I. and Gouyon, P.-H. 1997. Evolution of migration rate and other traits: the metapopulation effect. In *Metapopulation Biology: Ecology, Genetics and Evolution* (I. Hanski and M.E. Gilpin, eds.), pp. 293–323. San Diego, CA: Academic Press.

Ouborg, N.J., Biere, A. and Mudde, C.L. 2000. Inbreeding effects on resistance and transmission-related traits in the *Silene–Microbotryum* pathosystem. *Ecology*, **81**: 520–531.

Pettersson, T.M., Giles, B.E., Carlsson-Granér, U. and Elmqvist, T. 2000. Patterns of *Microbotryum violaceum* spore dispersal and disease spread in natural populations of *Silene dioica*. In *Spread of Anther-smut Disease in Natural Populations of Silene dioica* (T.M. Pettersson, ed.). Umeå: Department of Genetics, Umeå University.

Thompson, J.N. 1999. Specific hypotheses on the geographic mosaic of coevolution. *Am. Nat.*, **153**: S1–S14.

Thrall, P.H. and Antonovics, J. 1995. Theoretical and empirical studies of metapopulations: population and genetic dynamics of the *Silene–Ustilago* system. *Can. J. Bot.*, **73**: S1249–S1258.

Thrall, P.H. and Burdon, J.J. 1997. Host–pathogen dynamics in a metapopulation context: the ecological and evolutionary consequences of being spatial. *J. Ecol.*, **85**: 743–753.

Thrall, P.H. and Burdon, J.J. 1999. The spatial scale of pathogen dispersal: consequences for disease dynamics and persistence. *Evol. Ecol. Res.*, **1**: 681–701.

Thrall, P.H. and Burdon, J.J. 2002. Evolution of gene-for-gene systems in metapopulations: the effect of spatial scale of host and pathogen dispersal. *Plant Path.*, **51**: 169–184.

Thrall, P.H. and Jarosz, A.M. 1994a. Host–pathogen dynamics in experimental populations of *Silene alba* and *Ustilago violacea*. I. Ecological and genetic determinants of disease spread. *J. Ecol.*, **82**: 549–559.

Thrall, P.H. and Jarosz, A.M. 1994b. Host–pathogen dynamics in experimental populations of *Silene alba* and *Ustilago violacea*. II. Experimental tests of theoretical models. *J. Ecol.*, **82**: 561–570.

Thrall, P.H., Biere, A. and Antonovics, J. 1993. Plant life history and disease susceptibility: the occurrence of *Ustilago violacea* on different species within the Caryophylaceae. *J. Ecol.*, **81**: 489–498.

Thrall, P.H., Godfree, R. and Burdon J.J. 2003. Influence of spatial structure on pathogen colonisation and extinction: a test using an experimental metapopulation. *Plant Path.*, **52**: 350–361.

Van Putten, W.F., Biere, A. and Van Damme, J. 2003. Intraspecific competition and mating between fungal strains of the anther-smut *Microbotrym violaceum* from the host plants *S. latifolia* and *S. dioica*. *Evolution*, **57**: 766–776.